

# A novel approach to employ $\text{Li}_2\text{MnSiO}_4$ as anode active material for lithium batteries

V. Aravindan · K. Karthikeyan · S. Amaresh ·  
H. S. Kim · D. R. Chang · Y. S. Lee

Received: 24 June 2010 / Revised: 31 August 2010 / Accepted: 15 September 2010 / Published online: 27 October 2010  
© Springer-Verlag 2010

**Abstract** In the present paper, we describe utilization of cathode active material as anode active material, for example,  $\text{Li}_2\text{MnSiO}_4$ . The lithium manganese silicate has been successfully synthesized by solid-state reaction method. The X-ray diffraction pattern confirms the orthorhombic structure with  $Pmn2_1$  space group. The Li/Li<sub>2</sub>MnSiO<sub>4</sub> cell delivered the initial discharge capacity of 420 mA $\text{h}^{-1}$ , which is 110 mA $\text{h}^{-1}$  higher than graphitic anodes. The electrochemical reversibility and solid electrolyte interface formation of the Li<sub>2</sub>MnSiO<sub>4</sub> electrode was emphasized by cyclic voltammetry.

**Keywords** Li<sub>2</sub>MnSiO<sub>4</sub> · Anodes · Adipic acid · Solid-state reaction · Cyclic voltammetry

**PACS** 82.47.Aa · 82.45.Fk · 82.47.-a · 72.80.Tm

## Introduction

Carbonaceous materials have dominated as anodes for lithium ion batteries since commercialization in early 1990s by Sony, although such materials offered lower theoretical capacities (for example, graphite 372 mA $\text{h}^{-1}$ ) [1]. Transition metal oxides and their alloys were most widely investigated as possible alternative for the place of carbonaceous anodes. In addition, the transition metal elements afforded a high theoretical capacity, which are many folds higher than carbonaceous anodes. However, high irreversible capacity loss (ICL) during the conversion reaction and higher operating voltage restricts the possibility of using them in practical cells. In the case of alloy-based anodes, a large volume variation during alloying/dealloying process which severely affects the cycling stability, further cracking, and crumbling also possible during such process [2, 3]. Thus, it is necessary to search for new anode candidates for lithium ion batteries that are environmental friendly.

Utilization of cathode active materials into negative electrodes is the hot topic of research today. In the case of cathodes, the material should act as reservoir for the Li<sup>+</sup> ions; however, it acts as a buffer medium during the anodic process. For example, in LiFePO<sub>4</sub>, more than 90% of the theoretical capacity (170 mA $\text{h}^{-1}$ ) has been achieved when used as cathode. The insertion/extraction of lithium ions, i.e., oxidation/reduction, takes place around 3.4–3.6 V and provides the higher operating voltage. At the same time, LiFePO<sub>4</sub> exhibited the initial discharge capacity of 620 mA $\text{h}^{-1}$  while testing its anodic performance with coulombic efficiency around 100% [4]. In the same line, for the first of its kind, lithium orthosilicate material (e.g., Li<sub>2</sub>MnSiO<sub>4</sub>) has been subjected to investigate as an anode material for lithium batteries. The advantage of using such

V. Aravindan · K. Karthikeyan · S. Amaresh · Y. S. Lee (✉)  
Faculty of Applied Chemical Engineering,  
Chonnam National University,  
Gwangju 500-757, South Korea  
e-mail: leeys@chonnam.ac.kr

H. S. Kim · D. R. Chang  
Korea Institute of Industrial Technology,  
Gwangju 500-480, South Korea

*Present Address:*  
V. Aravindan  
Energy Research Institute,  
Nanyang Technological University,  
Singapore 639798, Singapore  
e-mail: aravind\_van@yahoo.com

silicate groups are low cost, high theoretical capacity, environmental benignity, and ease to prepare [5–9].

## Experimental

Solid-state reaction was employed to prepare the  $\text{Li}_2\text{MnSiO}_4$  powders. High-purity analytical grades of  $\text{LiOH}\cdot\text{H}_2\text{O}$  (Junsei 95%),  $\text{MnCO}_3$  (Aldrich, USA, 99.9%), and  $\text{SiO}_2$  (Aldrich, 99.9%) were used as the starting materials. In order to prevent the agglomeration of the particles during the synthesis, an adipic acid (Aldrich, 99%) has been chosen as a chelating agent, which was fixed at 0.2 mol against the total metal ion present in the compound. The stoichiometric amounts of starting materials with gelating agent were fine ground and heat treated at 400 °C for 4 h under air atmosphere. The resultant product was fine ground using mortar and pestle and placed in the tubular furnace at 900 °C for 12 h under Ar atmosphere for the final calcination process to yield the  $\text{Li}_2\text{MnSiO}_4$  powder.

The structural properties of  $\text{Li}_2\text{MnSiO}_4$  were studied by using X-ray diffractometer (Rigaku, Rint 1000, Japan) with  $\text{Cu-K}\alpha$  as a radiation source. Morphological features were investigated by scanning electron microscope (Hitachi, S-4700, Japan). Electrochemical profiles of  $\text{Li}_2\text{MnSiO}_4$  were performed by CR 2032 coin cell at ambient temperature. The negative electrode composed the accurately weighed 20 mg of active materials ( $\text{Li}_2\text{MnSiO}_4$ ), 3 mg of conductive additive (ketjen black), and 3 mg of binder (teflonized acetylene black). The mixture was pressed on a 200 mm<sup>2</sup> stainless steel mesh, serving as the current collector under a pressure of 300 kg/cm<sup>2</sup>, and dried at 130 °C for 5 h in an oven. The metallic lithium served as both reference and counter-electrodes. The cell was separated by a porous polypropylene film (Celgard 3401) filled with the conventional electrolyte solution (1.0 M  $\text{LiPF}_6$  in EC/DMC (1:1 v/v, Techno Semichem, Korea). The cyclic voltammetry (CV) and electrochemical impedance spectroscopy (EIS) studies were performed using SP-150, Bio-Logic, France electrochemical work station. The cycling studies were carried out between 0.0 and 3.0 V in galvanostatic mode at ambient temperature using WBCS 3000, Won-A-Tech, Korea.

## Result and discussion

Powder X-ray diffraction (XRD) pattern of  $\text{Li}_2\text{MnSiO}_4$  electrode material is given in Fig. 1. The XRD pattern shows the well-defined sharp intense reflections, which indicate the highly crystalline nature of the synthesized  $\text{Li}_2\text{MnSiO}_4$ . The crystalline peaks are suggesting the orthorhombic structure with  $Pmn2_1$  space group. The presence of impurity phases like  $\text{MnO}$  and less amount of

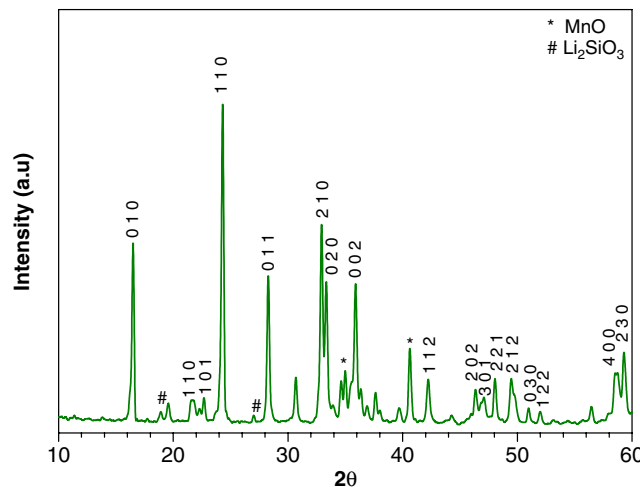


**Fig. 1** X-ray diffraction pattern of  $\text{Li}_2\text{MnSiO}_4$

$\text{Li}_2\text{SiO}_3$  are unavoidable during the synthesis process. A similar kind of impurity phases are noticed by the researchers during the synthesis of  $\text{Li}_2\text{MnSiO}_4$  powders by various approaches [5–10]. Abnormal pressure conditions provides the  $\text{MnO}$  and  $\text{Li}_2\text{SiO}_3$  free  $\text{Li}_2\text{MnSiO}_4$  phase. However, the obvious amount of  $\text{Mn}_2\text{SiO}_3$  phase could be inevitable under such conditions by de Dompablo et al. [11]. Moreover, the presence of  $\text{Mn}_2\text{SiO}_3$  phase is much higher than those of  $\text{MnO}$  present in the conventional synthesis. Earlier reports and present study shows that the preparation of phase pure  $\text{Li}_2\text{MnSiO}_4$  is a complicated one.

Morphological pictures of the synthesized  $\text{Li}_2\text{MnSiO}_4$  are analyzed by scanning electron microscopy (SEM) as shown in Fig. 2. The SEM image results connote the uneven size (submicrometer) morphology of the  $\text{Li}_2\text{MnSiO}_4$  particles synthesized by solid-state reaction method. Furthermore, the appearances of small-size particles are also seen along with the larger-size particles. It is well known that controlling growth of particle size/morphology by a solid-state reaction method is a very complex process.

The electrochemical performances of  $\text{Li}_2\text{MnSiO}_4$  against lithium reference electrode at ambient temperature are represented in Fig. 3. The cycling performances were carried out between 0 and 3 V at constant current density of C/20 galvanostatically. The  $\text{Li}_2\text{MnSiO}_4/\text{Li}$  cell presents the initial discharge capacity of  $420 \text{ mAh g}^{-1}$ . The initial discharge capacity of  $\text{Li}_2\text{MnSiO}_4$  electrode is  $110 \text{ mAh g}^{-1}$  higher than commercially graphitic anode ( $372 \text{ mAh g}^{-1}$ ) [12]. In the second cycle, the discharge capacity drastically reduced from 420 to  $181 \text{ mAh g}^{-1}$ . This reduction in capacity may be believed for the formation of solid electrolyte interface (SEI) especially at lower potentials. Generally, carbonaceous materials actively involved to the formation of SEI at lower potentials. Herein, the carbonaceous additives like adipic acid (it is carbonized during the calcination) and

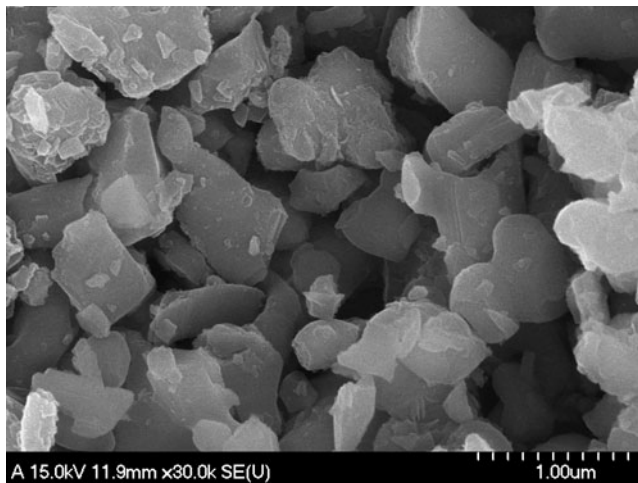


**Fig. 2** Scanning electron microscopic images of  $\text{Li}_2\text{MnSiO}_4$

conductive additive (ketjen black) effectively played a vital role for SEI formation [13, 14]. The SEI is necessary for the safe operation of the lithium cell during the prolonged cycling. Moreover, SEI prevents the unwanted side reaction with electrolyte counterparts. In the case of carbon-based materials, the columbic efficiency is around 100% except

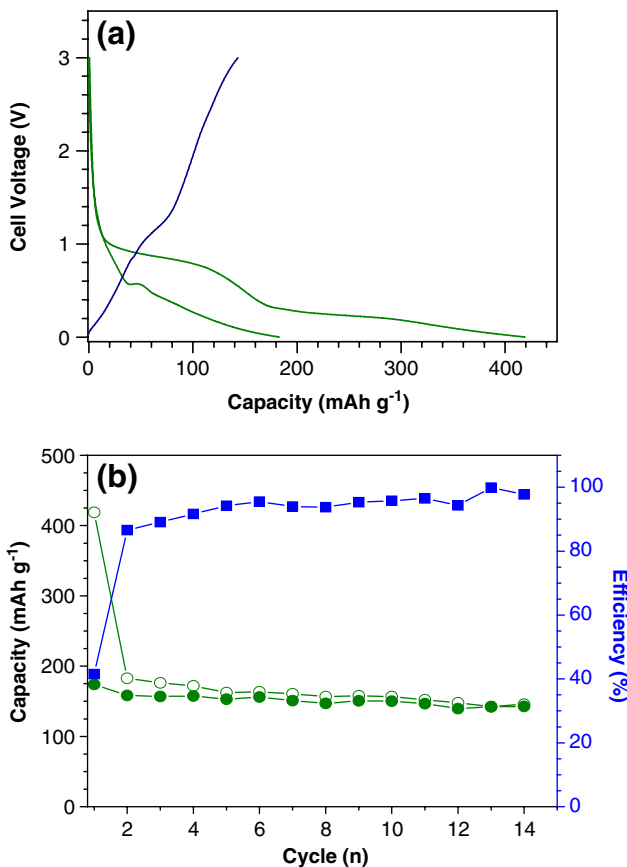


**Fig. 3** Electrochemical performance of  $\text{Li}_2\text{MnSiO}_4/\text{Li}$  cell **a** charge-discharge and **b** cycling profile (open circles for discharge capacity, filled circles for charge capacity, and squares for efficiency)

for the initial cycle, which indicates that such materials act as a buffer during intercalation/deintercalation process. However,  $\text{Li}_2\text{MnSiO}_4$  electrodes exhibited coulombic efficiency over 95%. This result suggests that  $\text{Li}_2\text{MnSiO}_4$  host material, which acts as the buffer host during discharge, provides enhanced columbic efficiency.

Generally, kinetic properties of lithium insertion/deinsertion properties can be effectively studied by cyclic voltammograms (CV). A family of voltammograms is given in Fig. 4 between the potential range of 0–3.5 V Vs  $\text{Li}/\text{Li}^+$  at ambient temperature with the scan rate of 0.1 mV/s. The operating potential covers the irreversible interactions between the host, lithium, and the electrolyte counterparts [13]. Moreover, this potential range is representative of the process at the anode under the normal battery operating conditions. In the first sweep, the cathodic peak around 0.56 V is representing the formation electronically insulating and ionically conducting SEI. Typically, the reversible lithium insertion and deinsertion processes takes place potentials below 0.5 V (versus  $\text{Li}/\text{Li}^+$ ). After the first cycle, the reduction in the intensities of the  $\text{Li}^+/\text{Li}$  potential indicates the involvement of lithium ions in the surface film formation, i.e., SEI [14]. Almost-stable voltammograms are observed from the subsequent cyclings, except for the first cycle. This confirms good reversibility of the  $\text{Li}_2\text{MnSiO}_4$  electrodes during lithium insertion/deinsertion process and corroborates cycling studies.

## Conclusion

The anodic performance of the  $\text{Li}_2\text{MnSiO}_4$  electrodes was herein demonstrated. The cell experienced the initial discharge capacity of  $420 \text{ mAh g}^{-1}$ , which is well ahead of commercially available graphitic anodes. The formation

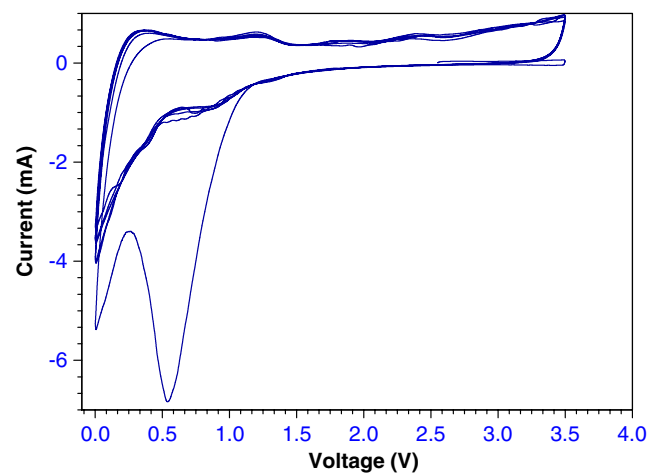


**Fig. 4** Cyclic voltammograms of  $\text{Li}_2\text{MnSiO}_4$  electrodes, when metallic lithium serves as counter and reference electrodes with the scan rate of 0.01 mV/s

of SEI and reversibility has been confirmed by cyclic voltammetric measurements. The XRD and SEM analyses were conducted to analyze the structural and morphological features, respectively.

**Acknowledgments** The authors gratefully acknowledge the supports by “Advanced materials and components project in Gwangju” funded by Korea Institute of Industrial Technology (KITECH).

## References

1. Arico AS, Bruce PG, Scrosati B, Tarascon JM, Schalkwijk WV (2005) *Nat Mater* 4:366
2. Bruce PG, Scrosati B, Tarascon JM (2008) *Angew Chem Int Ed* 47:2930
3. Shukla AK, Kumar TP (2008) *Curr Sci* 94:314
4. Kalaiselvi N, Doh CH, Park CW, Moon SI, Yun MS (2004) *Electrochem Commun* 6:1110
5. Nyten A, Abouimrane A, Armand M, Gustafsson T, Thomas JO (2005) *Electrochem Commun* 7:156
6. Dominko R, Bele M, Gaberšček M, Meden A, Remškar M, Jamnik J (2006) *Electrochem Commun* 8:217
7. Kokalj A, Dominko R, Mali G, Meden A, Gaberscek M, Jamnik J (2007) *Chem Mater* 19:3633
8. Dominko R (2008) *J Power Sources* 184:462
9. Liu W, Xu Y, Yang R (2009) *J Alloy Compd* 480:L1
10. Dominko R, Arcon I, Kodre A, Hanzel D, Gaberscek M (2009) *J Power Sources* 189:51
11. de Dompablo MEA, Dominko R, Amores JMG, Dupont L, Mali G, Ehrenberg H, Jamnik J, Moran E (2008) *Mater Chem* 20:5574
12. [http://en.wikipedia.org/wiki/Lithium-ion\\_battery](http://en.wikipedia.org/wiki/Lithium-ion_battery)
13. Aurbach D, Talyosef Y, Markovsky B, Markevich E, Zinigrad E, Asraf L, Gnanaraj JS, Kim HJ (2004) *Electrochim Acta* 50:247
14. Gnanaraj JS, Zinigrad E, Asraf L, Sprecher M, Gottlieb HE, Geissler W, Schmidt M, Aurbach D (2003) *Electrochem Commun* 5:946